CHAPTER 122

Sediment Suspension due to Large Scale Eddies
in the Surf Zone

by

Kazuo NADAOKA, Seizo UENO and Tatsuyuki IGARASHI

Dept. Civil Eng., Tokyo Institute of Technology
O-okayama 2-12-1, Meguro-ku, Tokyo 152, JAPAN

ABSTRACT

     Laboratory experiments using a fiber-optic LDV system
and a small pressure transducer have been made to reveal
detailed characteristics of the velocity field in the surf
zone and its relationship to the sediment suspension with
special reference to the three-dimensional large scale
eddies referred to as "obliquely descending eddies", the
existence of which was recently revealed by Nadaoka (1986).
A conditional sampling technique has been used to find that
the obliquely descending eddies bring highly intermittent
intensive turbulence to the bottom with the large onshore-
ward momentum at the upper layer of the water and thus es-
sentially characterize the turbulent flow field in the surf
zone.   Visual observation and concentration measurements,
especially a coherence analysis of two data sets of concen-
tration close to the bottom, have shown that the sediment
suspension is mostly governed by such large scale eddies in
a wide extent of the surf zone; i.e., the eddies hit the
bottom and then lift up the sediment into suspension,
yielding the spot-like sediment cloud in accordance with the
three-dimensional eddy structure.

1. Introduction

     The effect of wave breaking is one of the most signifi-
cant factors for the coastal sedimentary process.   In this
respect, Miller (1976), Shibayama and Horikawa (1985), and
others have discussed sand suspension by the action of the
large scale vortices generated immediately after the wave
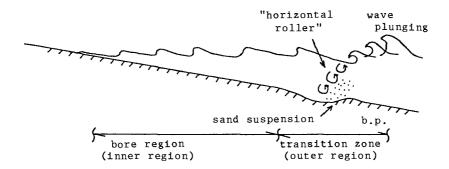plunging (Fig. 1).   The generation of such vortices, which

"horizontal   wave
  roller"   plunging

sand suspension   b.p.

bore region   transition zone
(inner region)   (outer region)

Fig. 1   "Horizontal rollers" and sediment suspension.
         (Miller 1976, Shibayama & Horikawa 1986, etc.)

obliquely descending
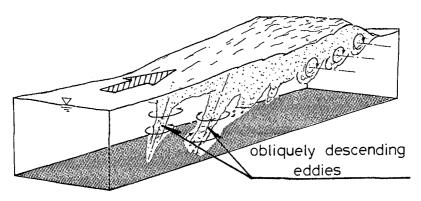   eddies

Fig.2   Schematic representation of the large scale eddy
        structure under breaking waves. (Nadaoka 1986)

are called "horizontal rollers", is a local phenomenon in
the sense that it is limited in space within the transition
zone or outer zone.   In another word, they don't affect
sediment suspension in the inner region or bore region.
     For spilling breaker condition, on the other hand,
Deigaard et al.(1986) have discussed the effect of the
turbulence originated from breaking water surface on the
vertical diffusion of the bottom sediment, by using the
transport equation for turbulent kinetic energy.   However,
the real physical process of the sediment suspension under
spilling breaker as well as turbulent bore has been not yet
well understood, mainly because of our limited knowledge of
the turbulent velocity field structure within the surf zone.
     Recently, Nadaoka(1986) has found the inherent eddy
structure of the breaking waves in a wide extent of the surf
zone.   That is, around the wave crest, dominant eddies have
nearly two-dimensional flow structure the axis of which is
parallel to the crest line, while behind the wave crest, the

flow structure changes quickly into that of obliquely down-
ward stretched eddies with strong three-dimensionality which
is referred to as "obliquely descending eddies" (Fig.2).
Therefore, it is worth to pay our attention to these ob-
liquely descending eddies, because they may act as possible
agitator of the bottom sediment in the surf zone.

    The main purpose of the present study is to clarify the
detailed characteristics of the turbulent velocity field in
the surf zone and its relationship to the sediment suspen-
sion with special reference to the "obliquely descending
eddies" under the turbulent bore.

2. Experimental Equipments and Procedure

    The wave channel used for the experiments was 0.6 m deep,
0.4 m wide and 20 m long, equipped with a flap-type wave
generator. The experiments were made both for a fixed bed
and a movable bed. In the former case, a wooden slope of 1
on 20 was installed at one end of the channel and in the
latter ground coal of 0.21mm in median diameter and of 1.45
in its specific weight was placed with the depth of 15cm on
the slope, as shown in Fig.3. The use of the ground coal
for the bed material was to suppress the generation of the
ripples under the wave action as much as possible, because
in the natural surf zone condition the ripples is hardly
developed.

    The experiment was carried out under the condition of
wave period $T=1.27$s, equivalent offshore wave height $H_0'=15.5$
cm, offshore wave steepness $H_0'/L_0=0.061$. Regular waves
generated by the wave maker produced a spilling-type
breaker, the depth and wave height of which, h_b and H_b, were
16.7 cm and 14.7 cm, respectively. It should be noted that,
under the spilling breaker condition, there exists no
horizontal roller.

    Horizontal and vertical velocity components, u and w,
were measured with a two-component fiber-optic laser-Doppler
velocimeter of back-scattered fringe mode (FLV, Hino et al.,
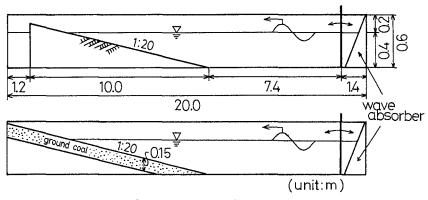1984). The water surface fluctuation η was measured with a

Fig.3   Experimental equipment.

capacitance-type wave gauge at right above the velocity mea-
suring point which was located at h/h_b =0.67 (h is the still
water depth). At the measuring section, breaking waves were
confirmed to be well developed into so-called "turbulent
bore".   A small pressure transducer of 1 cm in diameter, 3
mm in thickness and 1 kHz in its frequency response was used
for the measurement of bottom pressure fluctuation at the
measuring section. The concentration of the suspended bottom
sediment for the movable bed experiment was measured by a
light-attenuation-type sensor, the position of which was
manipulated to be kept at nearly the same height above the
bottom through the movable bed experiment.

3. Characteristics of Velocity Field Associated with Oblique Eddies

3.1 Intermittent structure of bottom turbulence and pressure fluctuation

     Figure 4 shows the phase-averaged distribution of the
turbulence intensity u' and w' at the several heights z
above the bottom.   The origin of the horizontal axis cor-
responds to the phase of the zero-up crossing point of the
water surface profile.   The values indicated were calculated
by averaging about 200 records of the high-frequency veloci-
ty component data which is obtained through a moving-average
filter with a averaging time of 0.1 s.   We can see in this
figure that the dependence of the turbulence intensity on
the phase variation as a whole is not so distinct, though
the turbulence intensity at z = 6.7cm slightly increases
around the phase of wave crest.   Especially, the turbulence
intensity close to the bottom is almost uniform except the
region around the phase of the wave crest, where the inten-
sity becomes larger probably corresponding to the increase
of the orbital velocity.
     Figure.5, on the other hand, is a typical example showing
the raw data of the water surface fluctuation η immediately
above the velocity measuring point, the bottom pressure
fluctuation p, and the velocity fluctuation u and w close to
the bottom (z=0.7cm).   In this figure, the bottom turbulence
occurs not uniformly, but appears in a quite intermittent
manner with the bottom pressure disturbances at the instants
indicated by the arrows.   Further, we should note that such
an intermittent occurrence of the bottom turbulence can be
found not under the wave crest, but around the phase of the
the zero-down crossing point.   This means that these inter-
mittent turbulence is not caused by the bottom shear stress
due to orbital wave motion.

3.2 Conditional sampling analysis of velocity field associated with the oblique eddies

     Comparison between Figs. 4 and 5 leads us to the idea
that the intermittent characteristics of the bottom turbu-
lence may be lost through the averaging process by the usual
phase-averaged method because of the random occurrence of
the intensive bottom turbulence, as shown in Fig.5.
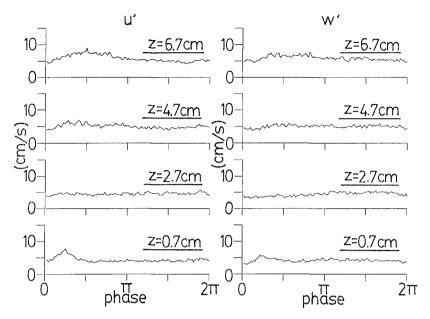   Considering the occurrence of such a highly intermittent

Fig.4   Distributions of phase-averaged turbulence intensity
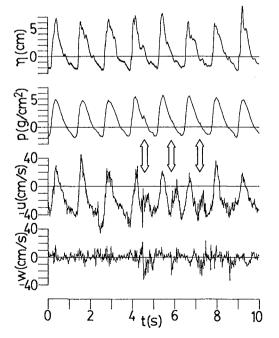u' and w'.

Fig.5   An example of time series of η, p, u and w.

bottom turbulence behind the wave crest, we can expect that
these disturbance is caused by the action of the obliquely
descending eddies mentioned first. The results of the visual
observation of the eddy evolution seemed to support this
expectation.   To confirm this point more quantitatively, we
have investigated the flow structure related to the inter-
mittent bottom disturbances by applying a conditional sam-
pling technique.

     In Fig. 5, we can find also that the pressure disturbance
occurs not so frequently as compared with the velocity
disturbances. Its possible explanation is that the pressure
disturbance occurs only at the instant when the pressure
gage is directly hit by an obliquely descending eddy.   Con-
sidering this characteristics of the pressure record, we can
utilize it as a trigger signal for the conditional sampling
to detect distinctively the velocity data corresponding to
the intermittent bottom turbulence.   Namely, by inspecting
whether the magnitude of the pressure disturbance exceed the
prescribed threshold level or not, we can classify each
individual wave record separated by the zero-up crossing
method into conditionally sampled or rejected records.   The
scanning of the pressure disturbance for the conditional
sampling was done within the phase interval $[\pi/2, 3\pi/2]$ of
each individual wave record, because the apparent pressure
fluctuation calculated by the moving- average method may
emerge in the phase intervals $[0, \pi/2]$ and $[3\pi/2, 2\pi]$
through the effects of the water surface fluctuation around
the wave crest and of the higher harmonics due to the wave
nonlinearity (Fig.6).   The number of the wave records
obtained through this conditional sampling is about 50, 1/10
of the total wave records.

     Figure 7 represents the phase-averaged distribution of
the turbulence intensity u' and w', where the solid and
broken lines correspond to the conditionally sampled and
rejected data, respectively.   We can clearly see in this
figure that the turbulence intensity of the sampled data at
the most upper measuring point attains relatively large
value around the wave crest and this intensive turbulence
propagates obliquely downward as indicated by the arrows,
while the turbulence intensity of the rejected data exhibits
no appreciable dependence on the phase variation.   This
means that the obliquely descending eddies bring intensive
turbulence to the bottom behind the wave crest.

     Figure 8 shows another result of the conditional sampling
analysis where the phase-averaged distributions of the mean
velocity, $<u>$ and $<w>$, of the conditionally sampled and no-
conditioned data are represented by the full and broken
lines, respectively.   In this figure, we can recognize that,
in the large turbulence regions, both the onshoreward and
the downward mean velocities are enhanced in the sampled
records.   This fact is directly related with the increase of
the downward transport of the onshoreward momentum as
described in what follows.

     The left and right figures in Fig. 9 represent the phase-
averaged distributions of the momentum transport for the
sampled and rejected records, respectively.   The solid lines
indicate the phase-averaged product of the horizontal and
the vertical velocity fluctuation, $<(u-\bar{u})\cdot(w-\bar{w})>$, where the
over bar means an operator to take a time average. Comparing
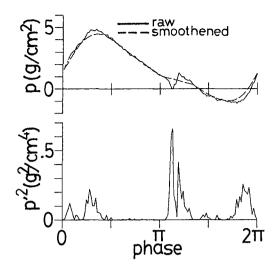
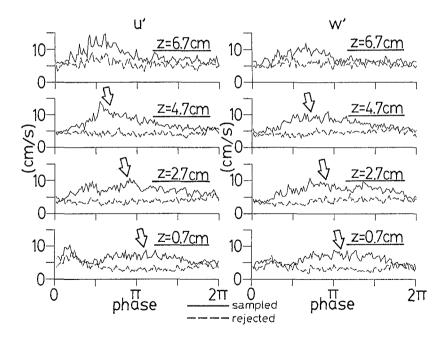Fig.6   Raw and smoothened data of p. p' is the difference between these two data.

Fig.7   Phase-averaged distributions of the turbulence intensity u' and w' for conditionally sampled and rejected records.
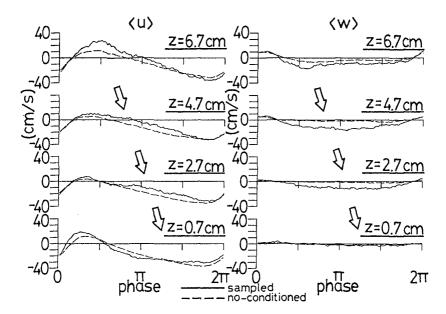
Fig.8 Distributions of phase-averaged velocity $<u>$ and $<w>$ for conditionally sampled and no-conditioned records.
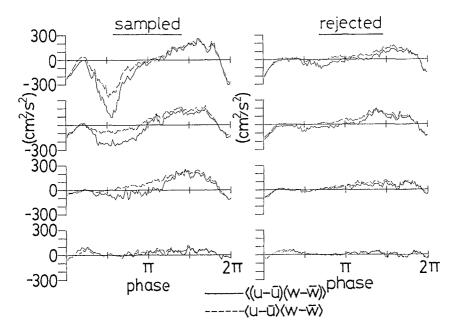

Fig.9 Distributions of phase-averaged momentum flux for conditionally sampled and rejected records.

the left and the right figures, we can clearly see that the
momentum transport of the sampled records considerably
increases as a whole.
   The broken lines, on the other hand, represent the product
of the phase-averaged horizontal and vertical velocity
fluctuation, $<u-\bar{u}>\cdot<w-\bar{w}>$.   The difference between the solid
and broken lines corresponds to the turbulent momentum
transport. The fact that the difference becomes large in the
highly turbulent regions means that the production of an
appreciable magnitude of the Reynolds stress accompanies the
evolution of the oblique eddies.

     In summary, all of these results are consistent with the
following conceptual model based on the obliquely descending
eddies.   That is, the eddies transport the intensive turbu-
lence obliquely downward with the large onshoreward momentum
at the upper layer of the water, and then brings the highly
intermittent turbulent velocity and pressure fluctuation to
the bottom.
     Considering these results obtained through the fixed-bed
experiments, we can easily expect that this eddy action to
the bottom plane causes sediment suspension in a wide extent
of the surf zone.   To obtain more definite results on the
relationship between the eddy action and resultant sediment
suspension, we have   made movable-bed experiments, as
described as follows.

4. Relation between the Obliquely Descending Eddies and the
   Sediment Suspension

4.1 On-offshore distribution of the mean sediment
    concentration close to the bed

     The on-offshore distributions of the time-averaged
concentration $\bar{c}$ both at z=0.5cm located within the bedload
layer and at z=1.0cm just above the layer are shown in the
bottom of Fig.10.   The values indicated were based on the
data measured during the time interval of about 70s from the
instant when the wave set-up was established until the time
when the sediment ripples were generated.   The initial
bottom surface configuration was smoothened for each run.
   The upper figure, on the other hand, shows the distribution
of the bottom turbulence intensity w' and of the amplitude
of orbital velocity u_m normalized by the linear long wave
speed at the breaking point. These values of w' and u_m are
those measured at $z=0.7$cm in the fixed-bed experiments.
Unlike for the values of the turbulence intensity indicated
in Figs. 4 and 7, the averaging time for the numerical
filtering of the raw data is the time of the incident wave
period, because the vertical component of the near-bottom
velocity contains negligibly small magnitude of the orbital
velocity as compared with the turbulence.   Hence $\bar{w}'$-values
so obtained include almost all contribution of the oblique
eddy motion.
     Comparing the shape of these distributions each other,
we can recognize that the sediment concentration level $\bar{c}$ in
the bed load layer correlates well to u_m, while $\bar{c}$ above the
layer varies in accordance with the bottom turbulence inten-

sity w'. This result suggests the close relationship between the sediment suspension and the action of the oblique eddies.
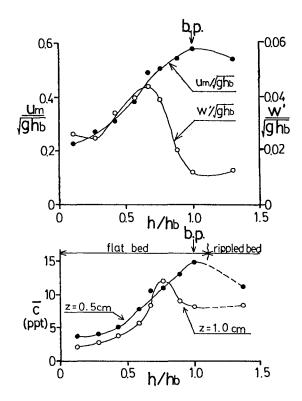

Fig. 10   Spatial distributions of mean concentration $\bar{c}$ at $z = 0.5$ and 1.0cm and those of bottom turbulence intensity w' and amplitude of orbital velocity u_m.

4.2 Visualization of the eddy evolution and the resultant occurrence of sediment suspension

To confirm this relationship from a visual aspect, we have taken some photos from a side wall of the wave channel. Photo 1 and Figure 11 are examples showing a sequence of pictures and their tracings around the velocity measuring section taken successively by a motor-driven 35 mm camera. The vertical rod shown in the photos is the stem of the sensor to measure the sediment concentration. The instants taking the photos are indicated by the arrows denoted by the alphabets of A to H in Fig. 12, where both the water surface elevation η and the bottom sediment concentration c at $z = 1.0$ cm at the velocity measuring section are represented. The records shown in Fig. 12 were those obtained immediately after the starting of the wave generator; thus the first
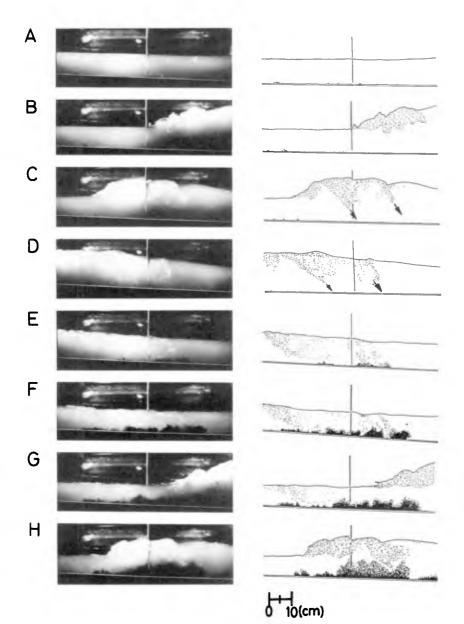
Photo 1 Development of obliquely descending eddies and sediment suspension.
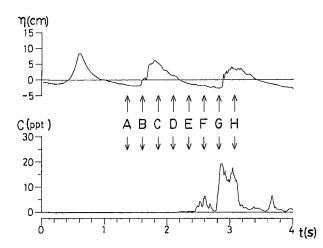
Fig.11 Tracing of Photo 1.

0　10(cm)

Fig.12   The instants taking the photos and the time
          histories of η and c.

wave indicated in the figure is a non-breaking wave.   The
figure indicates that the sediment concentration increases
not under the first non-breaking wave, but around the phase
of the trough of the second breaking wave.
        The brighter regions of the photos indicate the air
bubbles involved in the eddies, which are sketched in Fig.11
by the speckles.   The dark regions close to the bottom in E
to H, on the other hand, indicate the suspended sediment
cloud.   From these photos and figures, we can describe the
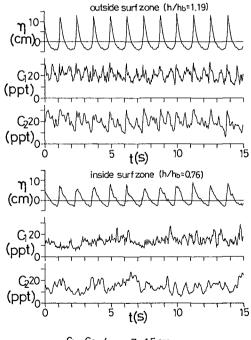process of the eddy development and associated sediment
suspension as follows.

(A)······   No appreciable sediment suspension can be found,
            though there exists the sediment movement due to
            sheet-flow.
(B)······   The horizontal eddies grow to appear in front of
            the bore crest.
(C)······   The eddies develope into the obliquely descending
            eddies behind the wave crest.   The sediment suspen-
            sion, however, cannot be found yet at this stage.
(D)······   The oblique eddies stretch toward the bottom as
            indicated by the arrows.
(E)······   Immediately after the instant when the eddies hit
            the bottom surface, the sediment suspension appears
            in the vicinity of the bottom.
(F)······   A large amount of the sediment is lifted up into
            suspension by the eddy action, increasing the
            concentration value as shown in Fig. 12.
(G)······   The sediment clouds migrate offshore with the
            backwash of the bore. And then they are convected
            upward by the heaving orbital motion preceding to
            the passage of the wave crest.
(H)······   The subsequent oblique eddies evolve toward the
            bottom.

4.3 3-D structure of suspended sediment cloud in the surf zone

The dependence of the sand suspension on the oblique eddies mentioned above may be confirmed more quantitatively by investigating the spatial structure of the suspended sand cloud; i.e, if the oblique eddies lift up the bottom sediment into suspension, the resultant sediment cloud will show the strong three-dimensionality with the horizontal scale comparable to that of the diameter of the eddies. So to investigate the spatial structure of the sediment cloud close to the bottom, we have measured simultaneously the sediment concentration c_1 and c_2 by the two probes aligning several distances apart in the direction perpendicular to the plane of the orbital wave motion.

Figure 13 shows the time histories of the water surface elevation η as well as c_1 and c_2 both outside and inside the surf zone. The values of c_1 and c_2 in this figure are those measured by the probes manipulated to keep their hights at 1.5cm above the bottom and separated with 4cm each other in the horizontal cross-channel direction.

The values of c_1 and c_2 outside the surf zone well correlate to each other and exhibit strong dependance on the phase variation with the two marked peaks within the one

outside surf zone (h/h_b=1.19)

inside surf zone (h/h_b=0.76)

$c_1 - c_2$ 4cm Z=1.5cm

Fig.13   An example of the time histories of η as well as c_1 and c_2 both outside and inside the surf zone.
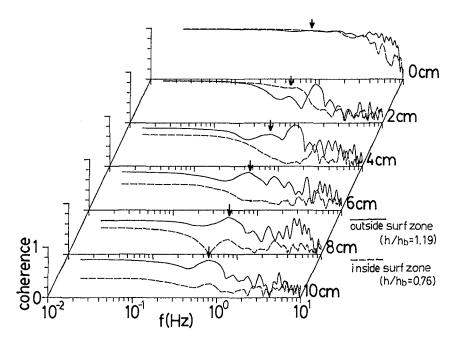
Fig.14   Coherence between bottom concentration records for
         several probe spacings.

wave period, though the high frequency component is slightly
losed in c_2 record as compared with c_1, because the frequen-
cy response of the probe for c_2 is lower than that for c_1.
The concentration variation inside the surf zone, on the
contrary, shows no definite phase-dependance, and the cor-
relation between these two records is rather poor.   These
facts suggest that the sediment suspension within the surf
zone is mostly governed by the turbulence, especially by the
obliquely descending eddies, generated with the wave break-
ing, though, in the outside of the surf zone, the wave fluid
motion is a unique action to the sediment suspension, which
is nearly two-dimensional phenomenon.
    Then to investigate the correlation structure between c_1
and c_2 more quantitatively, we have calculated the coherence
between c_1 and c_2.   The results are shown in Fig.14, where
the coherence values are   indicated for several probe
spacings with the horizontal axis of frequency f.   The data
used are those measured for the initially smoothened bed
during the time interval of about 80 s from the instant when
the wave set-up was established to the time when the
sediment ripples were generated.
    The coherence outside the surf zone denoted by full lines
retain high values even for the large probe spacings,
demonstrating two-dimensionality of sediment suspension
outside the surf zone. On the contrary, the coherence within
the surf zone represented by broken lines decreases rapidly

with the probe spacings. The decrease is most noticeable in
the frequency range from 0.8 to 5 Hz which is corresponding
to the period of the incident waves and its higher harmonics
and is comparable to the frequency of the eddy occurrence.
This means that the sediment suspension inside the surf zone
occurs in a quite spot-like manner and is consistent again
with the proposed model of sediment suspension by the
oblique eddies.

5. Conclusions

    The results and conclusions obtained in the present study
can be summarized as follows.

1) "Obliquely descending eddies" bring highly intermittent
turbulence to the bottom with the large onshoreward momentum
and thus essentially characterize the turbulent flow field
in the surf zone.

2) The eddies hit the bottom and then lift up the sediment
into suspension, yielding the spot-like sediment cloud in
accordance with the 3-dimensional eddy structure.

References

Deigaard, R., Fredsoe, J. and Hedegaard, I.B.(1986): Sus-
        pended sediment in the surf zone, Jour. of Waterway,
        Port, Coastal and Ocean Engineering, ASCE, Vol.112,
        No.1, pp.115-127.

Hino, M., Sawamoto, M., Yamashita, T., Hironaga, M. and
        Muramoto, T.(1984): Prototype 2-dimensional LDV
        adopting optical fibers, Laser-Doppler Velocimetry
        and Hot-Wire/Film Anemometry, Association for the
        Study of Flow Measurement.

Miller,R.L.(1976): Role of vortices in surf zone prediction:
        sedimentation and wave forces, Beach and Nearshore
        Sedimentation, Soc. Econ. Paleontol. Mineralog.,
        Spec. Publ. No. 23, pp.92-114.

Nadaoka, K.(1986): A fundamental stdy on shoaling and
        velocity field structure of water waves in the
        nesrshore zone, Doctoral Dissertation, Tokyo Inst.
        of Tech. (reproduced in Tech. Rept. of Dept. Civil
        Eng., Tokyo Inst. of Tech. No.36, pp. 33∿125, 1986.)

Shibayama, T. and Horikawa S.(1985): Sediment transport due
        to breaking waves, Proc. of 20th Int. Conf. on
        Coastal Eng., ASCE, pp.1509-1522.